  Bull. Chem. Soc. Jpn., 59, 551—556 (1986)

Electrolytic Recovery of Silver from Photographic Fixing Solutions with a Fluidized Bed Electrode

Isao SEKINE* and Hiroyuki ISHII
Faculty of Science and Technology, Science University of Tokyo, Yamazaki, Noda, Chiba 278
(Received January 17, 1985)

For an effective electrolytic recovery of silver from photographic fixing solutions, polarization measurements and potentiostatic electrolysis were carried out using active carbon as a fluidized bed electrode. The optimum conditions, determined by the electrolytic recovery, required a static bed height was 4 mm, a bed expansion rate 14%, and an initial set potential −0.84 V vs. SCE. The current efficiency in this case was about 75%, and the limiting concentration for recovery of silver was about 5 ppm. The electrolytic duration for recovery of the silver was reduced to about half by enlarging the electrolytic cell. Other products formed during the electrolysis were hydrogen sulfide (H_2S) and silver sulfide (Ag_2S). When silver deposited under the optimum conditions was dissolved in 5M-HNO_3 (1M=1mol dm^{-3}) of 100 ml, the recovery efficiency of the silver was about 75%.

Electrolytic recovery of metals with a fluidized bed electrode is favorable in dilute solutions. It is also known to be more effective than a fixed bed electrode.[1-4] Active carbon, which has an ability for physical adsorption and a better conductivity, has rarely been used in electrolytic recovery as material for a bed electrode.

In the present work, the effective electrolytic recovery of silver in the photographic fixing solution was investigated using active carbon. The various kinds of photographic fixing solutions contain relatively large amount of silver ion. Therefore, the recovery of silver is important from the viewpoint of saving natural resources. Moreover, the optimum conditions for carrying out effective potentiostatic electrolysis were determined by measuring the cathodic polarization curve and by electrolysis. Factors are the static bed height, the bed expansion rate, and the initial set potential. The effect of scale up of the electrolytic cell and the recovery efficiency of silver were also investigated. The product deposited on the cathode was identified by X-ray diffraction.

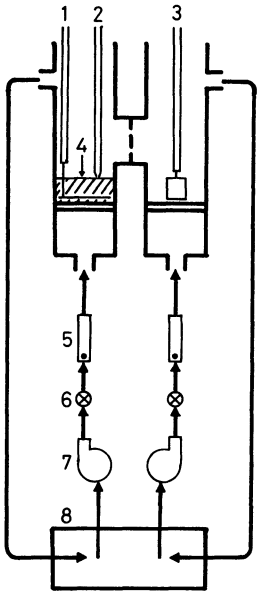

Fig. 1. Apparatus for electrolytic recovery of Ag. 1: Working electrode (Pt wire), 2: Reference electrode (SCE), 3: Counter electrode (Pt plate), 4: Fluidized bed electrode (active carbon), 5: Flow meter, 6: Valve, 7: Pump, 8: Tank in water bath.

Experimental

Cell and Electrode. The cell for the electrolytic recovery is shown in Fig. 1. The cell is made of acrylic resin. It has an H-type structure with an inside diameter of 26 mm or 18 mm. The diameter of both the inlet and the outlet for the solution was 7 mm. Anolyte and catholyte were divided by a diaphragm to prevent the electrolyte from mixing by natural convection. The electrolyte was filtered through a porous acrylic resin plate interposed at a point 35 mm up from the inlet through which the solution flows into the cell. The average particle diameter of the active carbon used as a fluidized bed electrode was 1.53 mm. The active carbon was used after immersion in distilled water for more than one day. The cathode was a spiral platinum wire of 0.5 mm diameter used as a feeder electrode on the porous acrylic resin plate, and the active carbon was placed on the feeder electrode. The anode was a platinum plate of 15×10 mm. Both anode and cathode were subsequently washed with ethanol, 1M-HNO_3 and 1M-HCl. The reference electrode was a saturated calomel electrode (SCE).

Electrolyte. The electrolyte was prepared by diluting tenfold a photographic fixing solution with distilled water. The electrolyte with a volume of 1 dm^3 was pumped to the cell from a tank maintained at 30 °C; the flow rate was controlled by a Teflon valve and was determined through a flow meter. Moreover, the electrolyte was circulated from the outlet of the cell to the tank, after it had fluidized the active carbon.

Polarization Measurement and Electrolysis. The measurements of the polarization curves were carried out by the potentiostatic method. The potential was changed stepwise from a natural electrode potential (NEP) to a less noble potential at a scan rate of 50 mV min^{-1}. The electrolytic recovery of silver was also carried out for 6 h by the potentiostatic method.

Concentration Determination of Silver Ion. The concentration of silver ion in the solution was determined by atomic absorption analysis. In this analysis, air-acetylene was used as a flame, and the wavelength of irradiation was 3281 Å for Ag. The concentration of silver ion was determined from

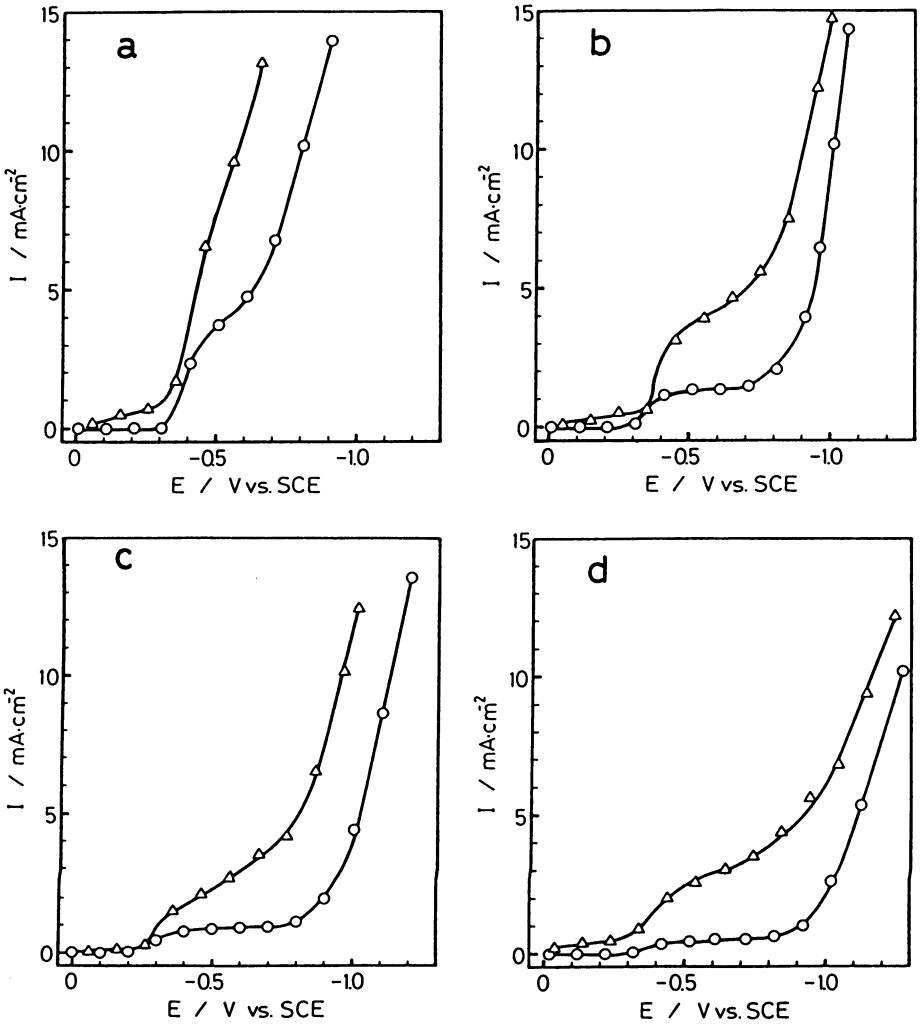

Fig. 2. Current density vs. potential curves for various dilution ratios, (a): 1/2, Ag^+ 2850 ppm, (b): 1/5, Ag^+ 1140 ppm, (c): 1/10, Ag^+ 570 ppm, (d): 1/20, Ag^+ 285 ppm.
—○—: feeder, —△—: 4 mm, 14%.

the calibration curve.

Analysis of Silver Sulfide. Silver sulfide as another product was deposited like a halo on the surface of the granular active carbon. This product was identified by X-ray diffraction. The wavelength of the irradiating X-ray was 1.9373 Å (Fe $K\alpha$).

Recovery Efficiency of Silver. To obtain the recovery efficiency of silver, the electrolysis was carried out under optimum conditions with a static bed height of 4 mm, a bed expansion rate of 14%, a set potential of −0.84 V vs. SCE and an electrolytic duration of 3 h. The amount of silver recovered from the photographic fixing solutions by electrolysis was about 0.5 g. In this case, the recovery of silver was stopped before the concentration of silver ion reached the lower limited value of about 5 ppm, because a large amount of silver sulfide was formed. The silver deposited on the active carbon was dissolved in 5M-HNO_3 of 100 ml for 2 h with stirring. The recovery efficiency of silver was obtained by the ratio of the dissolved silver (g) to the deposited silver (g).

Results and Discussion

Polarization Measurements. (I) Effect of Concentration: In the cell having an inside diameter of 26 mm, the polarization curves for the photographic fixing solutions diluted 2, 5, 10, and 20 times with water are shown in Fig. 2. These data were obtained by measurement under the following conditions: The static bed height of fluidized bed electrode was 4 mm, the bed expansion rate 14%, and the solution temperature 30±0.5 °C. In the case of the feeder electrode only, the flow rate of solution was 0.3 dm^3 min^{-1}. The current density on both the fluidized bed and the feeder electrode increases only with increasing concentration of silver. This can be explained by the fact that the bulk concentration of silver ion is directly proportional to the current. When the concentration of silver ion in the photographic fixing solution increases from 285 ppm in 20 times dilution to 2850 ppm in twofold dilution, the specific conductivity increases from 7500 to 53900 μS cm^{-1}, so that the current increases. Throughout the potential range, the current on the fluidized bed electrode is greater than that on the feeder electrode. Consequently, the

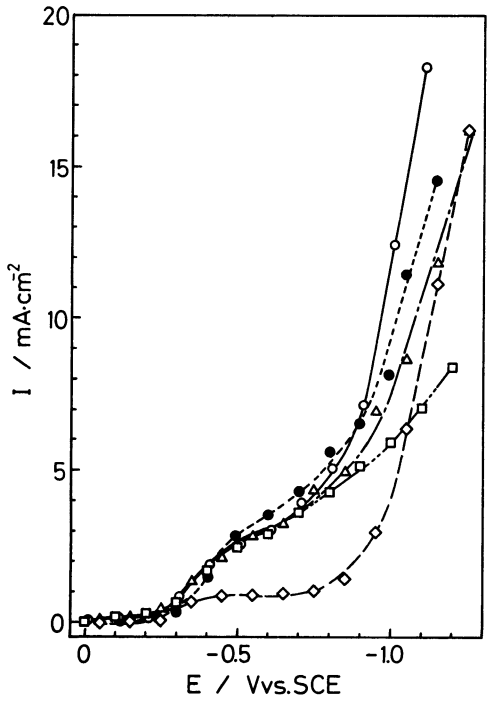

Fig. 3. Current density vs. potential curves for various static bed heights at expansion of 14%.
——○——: 4 mm, -·-△-·-: 8 mm, —-□—-: 12 mm, ——◇——: feeder, ----●----: 4 mm (inside diameter of 18 mm).

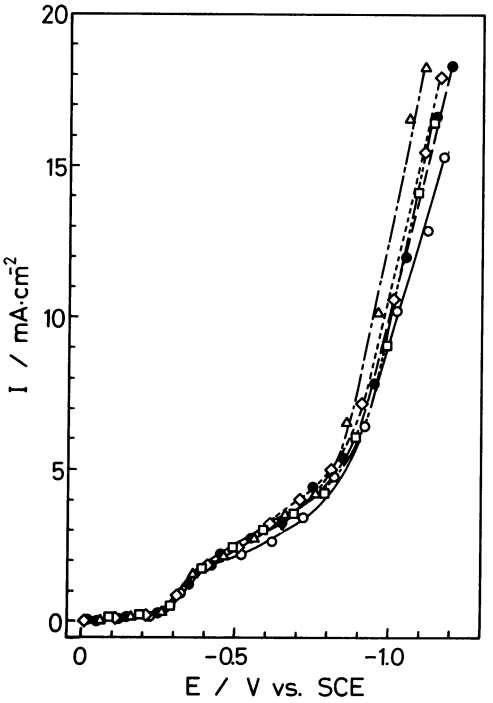

Fig. 4. Current density vs. potential curves for various bed expansions at bed height of 4 mm.
——○——: 10%, —-△—-: 14%, —-□—-: 17%, ---◇---: 20%, --●--: 30%.

fluidized bed would act as an effective electrode. However, the fluidized bed electrode was found to work effectively when the photographic fixing solution was diluted with water more than 10 times and the static bed height was 12 mm. This can be explained by the fact that the shape of the polarization curves obtained under these conditions resembled that in Fig. 2.

(II) Effect of the Static Bed Height: In a cell having an inside diameter of 26 mm, the polarization curves for static bed heights of 4, 8, and 12 mm, and for a feeder electrode only are shown in Fig. 3. These data were obtained at an expansion rate of the bed of 14% and a solution temperature of 30±0.5 °C. The current density decreases with increasing static bed height. As the ohmic drop in the fluidized bed electrode increases with increasing amount of active carbon, the decrease of the current density would be ascribed to the spread of potential distribution in the bed. When the static bed height was 4 mm, a fluidized bed electrode was more effective than a feeder electrode over all potential ranges. This current density was approximately the same as that with a small cell of 18 mm inside diameter. The optimum static bed height of the cells having inside diameters of 18 and 26 mm was 4 mm.

(III) Effect of Bed Expansion: In the cell having an inside diameter of 26 mm, the polarization curves for bed expansion rates of 10, 14, 17, 20, and 30% at a static bed height of 4 mm and a solution temperature of 30±0.5 °C are shown in Fig. 4. In all cases, a small difference in the current density was observed at less noble potentials than −0.8 V vs. SCE. However, the current density in the noble potential range less than −0.9 V increased steeply. These phenomena can be attributed to the evolution of H_2S and H_2.[5] In the less noble potential range below −0.8 V, the current density shows the highest value at a bed expansion rate of 14%. The current value is approximately the same at 17 and 20%, and lowest at 10 and 30%. In the case of a bed expansion rate smaller than 14%, the current density was small because the effective surface area of electrode was not spread sufficiently. In the range of 14—20%, the transfer to the cathode surface of the Ag^+ ion is promoted by the rotatory motion of the active carbon particles themselves, and the collision numbers among the particles as well as between the particles and the feeder are considerably increased. The charge transfer reaction is believed to proceed smoothly. Also, the thickness of the diffusion layer became smaller because of the flow of electrolyte; hence the current density increased.[6] Above 20%, the conductivity of the fluidized bed electrode deteriorates because the space rate of active carbon particles is increased. The amount of active carbon serving as an electrode was gradually diminished. As the resistance of the bed became progressively greater with increasing bed expansion rate, the current density is inferred to become smaller.[7] The current density with the cell of inside diameter of 26 mm did not differ significantly

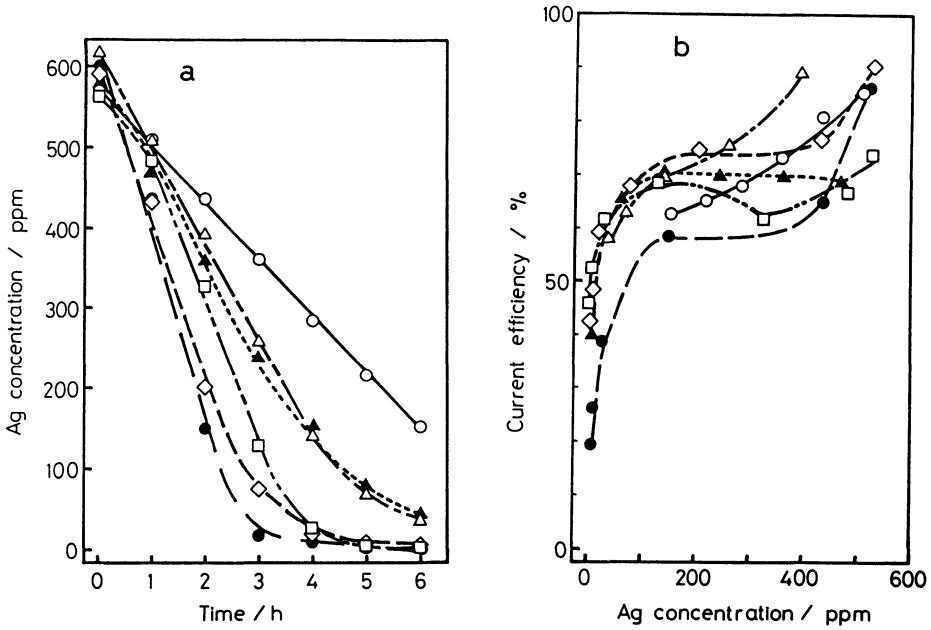

Fig. 5. (a) Change of concentration of silver ion as a function of time, and (b) current efficiency vs. concentration curves for various initial set potentials at bed bed height of 4 mm and expansion of 14%.
—○—: −0.60 V, —△—: −0.70 V, —□—: −0.80 V, —◇—: −0.84 V, —●—: −0.85 V, —▲—: −0.84 V (inside diameter of 18 mm).

from that for the cell of 18 mm inside diameter.

Macroelectrolysis. (1) Effect of Initial Set Potential: The relationship between the concentration of silver ion and the electrolytic duration at various set potentials is shown in Fig. 5(a), and the current efficiency in this case is shown in Fig. 5(b). These data were obtained for a static bed height of 4 mm, bed expansion rate of 14%, and solution temperature of 30±0.5 °C with the cell of inside diameter of 26 mm. The electrolytic duration for recovery of silver became much shorter as the set potential shifts to a less noble potential. The concentration of silver ion decreased linearly from about 600 ppm to about 100 ppm by electrolysis. At a concentration below about 100 ppm, the electrolytic duration for recovery of silver gradually increased. On enlarging the inside diameter of cell, the electrolytic duration for recovery of silver ion up to 50 ppm took about 5.8 h at the inside diameter of 18 mm, but it could be reduced to about 3.5 h in a cell of 26 mm diameter. On the other hand, at concentrations of silver ion up to about 100 ppm the current efficiency increased steeply with increasing concentration. At a concentration of silver ion above about 100 ppm, it was independent of the concentration and reached a value of about 60—75%. The low current efficiency in the concentration range up to about 100 ppm can be ascribed to the diffusion of silver ion in the dilute solution.[8] Such a tendency was similar to that described by Walker et al. for the electrolytic recovery of copper.[9] Moreover, the low current efficiency was due to the formation of other products such as H_2S and Ag_2S. The evolution of H_2S was observed at concentrations below about 100 ppm of silver ion, and at a negative set potential lower than −0.8 V vs. SCE. The H_2S evolution reaction[5] is considered to occur by

$$S_2O_3^{2-} + 2H_2O + 2e^- \longrightarrow H_2S + SO_3^{2-} + 2OH^- \quad (1)$$

Furthermore, a black powder was deposited on the cathode at all set potentials as the concentration of the silver ion decreased. The black powder was shown to be Ag_2S by X-ray diffraction analysis. The deposition reaction of silver from photographic fixing solutions is given as

$$Ag^+ + 2S_2O_3^{2-} \rightleftharpoons [Ag(S_2O_3)_2]^{3-} \quad (2)$$

$$Ag(S_2O_3)_2^{3-} + e^- \longrightarrow 2S_2O_3^{2-} + Ag \quad (3)$$

Then, this reaction competes further with the formation of silver sulfide as follows:[10]

$$H_2S \rightleftharpoons H^+ + HS^- \quad (4)$$

$$H_2S + 2[Ag(S_2O_3)_2]^{3-} \longrightarrow Ag_2S + 2H^+ + 4S_2O_3^{2-} \quad (5a)$$

or

$$HS^- + 2[Ag(S_2O_3)_2]^{3-} \longrightarrow Ag_2S + H^+ + 4S_2O_3^{2-} \quad (5b)$$

From both the recovery time and the current efficiency, it is concluded that the optimum set potential was −0.84 V vs. SCE, and that the limiting concentration of recovery was about 5 ppm. Further, when the inside

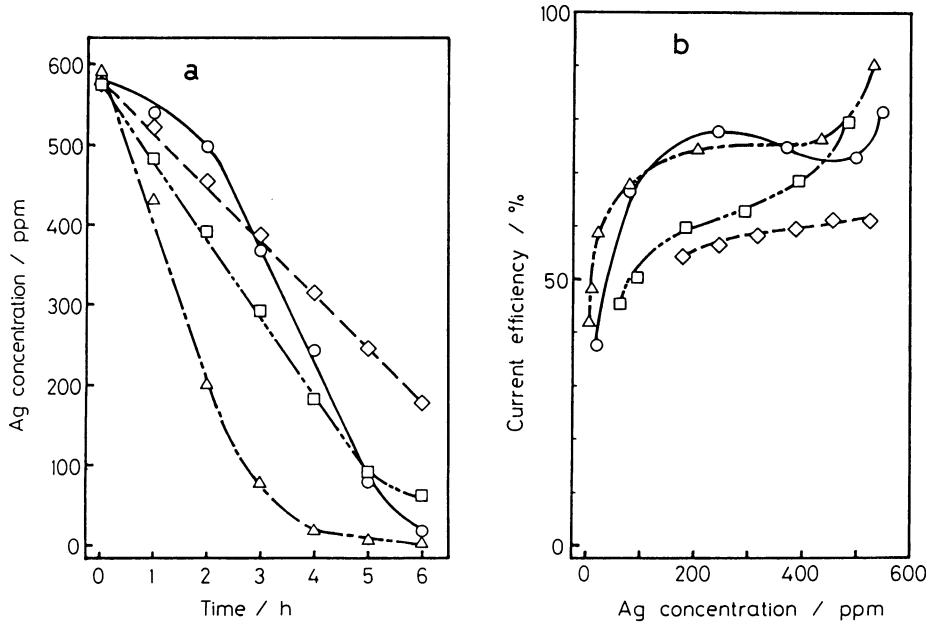

Fig. 6. (a) Change of concentration of silver ion as a function of time, and (b) current efficiency vs. concentration curves for various static bed heights at set potential of −0.84 V vs. SCE and expansion of 14%.
——○——: feeder only, —-△—-: 4 mm, —--□—--: 8 mm, --◇--: 12 mm.

diameter of the cell is enlarged from 18 mm to 26 mm, the electrolytic duration for recovery of silver became fairly short. However, the current efficiency for 26 mm was similar to that for 18 mm. In actual electrolysis, the electrolytic duration for recovery was found to be shorter as the electrode surface area is larger in the experimental range.

(II) Effect of Static Bed Height: In the cell having an inside diameter of 26 mm, the relationship between the concentration of silver ion and the electrolytic duration in various static bed heights is shown in Fig. 6(a). The current efficiency in such a run is shown in Fig. 6(b). The bed expansion rate was 14%, the initial set potential −0.84 V vs. SCE, and the solution temperature 30 °C. The electrolytic duration for recovery became shorter as the static bed height decreased. As shown in Fig. 3, the current density at less noble potential than −0.7 V vs. SCE became smaller in the order of 4, 8, and 12 mm of the bed height. Hence, the electrolytic duration for recovery was found to correspond to the result of the polarization measurement. The dependence of the electrolytic duration for recovery on the static bed height would be ascribed to the IR-drop as described previously. The electrolytic duration for recovery with the feeder electrode only was longer than that for the others with in about three hours. As seen in Fig. 3, the current density with the feeder electrode only was much smaller than that with the fluidized bed electrode. These results show that the electrolytic duration for recovery was long at the beginning of electrolysis. The value of the current efficiency decreased in the order of 4, 8, and 12 mm. However, silver sulfide was observed to produce in any bed height. Consequently, the optimum static bed height was 4 mm. The electrolytic duration for recovery of silver with the cell of inside diameter of 26 mm became shorter with decreasing static bed height resembling that obtained with the cell of inside diameter of 18 mm. Hence, the electrolytic duration for recovery was reduced as the inside diameter of the cell increased.

(III) Effect of Bed Expansion Rate: In the cell having an inside diameter of 26 mm, the relationship between the concentration of silver ion and the electrolytic duration in various bed expansion rates is shown in Fig. 7(a). The current efficiency in electrolysis with static bed height of 4 mm, set potential of −0.84 V vs. SCE, and solution temperature of 30± 0.5 °C is shown in Fig. 7(b). The electrolytic duration for recovery of silver was found to be almost independent of the bed expansion rate over the range of the experiment. Such a result would follow from the polarization curve in Fig. 4, because the current density did not change remarkably at various bed expansion rates. However, the current efficiency was optimal in a bed expansion rate of 14%. This may be ascribed to the increase of the effective surface area of the electrode, the decrease of the thickness of the diffusion layer, and the decrease of the bed resistance, as discussed above. At all bed expansion rates, H_2S and Ag_2S were observed to form as the concentration of silver ion decreased. From these results, it is concluded that the optimum bed expansion rate is 14%.

Yield of Silver. When silver deposited on active

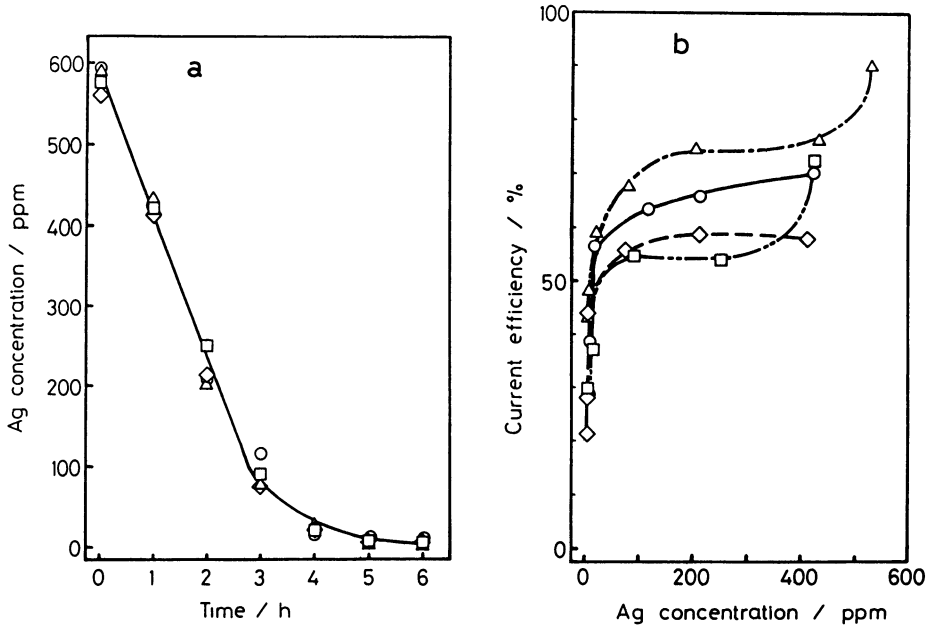

Fig. 7. (a) Change of concentration of silver ion as a function of time, and (b) current efficiency vs. concentration curves for various bed expansion rates at set potential of −0.84 V vs. SCE and bed height of 4 mm.
——○——: 10%, —-△—-: 14%, —--□—--: 20%, --◇--: 30%.

carbon was dissolved in 100 ml of 5M-HNO_3, the yield was about 75%. Silver of 25% could not be recovered, this may be attributed to the silver deposited inside of active carbon not being completely dissolved, and to silver isolated from the surface of the electrode as powdery Ag_2S being deposited on the inside of the pump, valve, and flowmeter.

The authors wish to thank Mr. Takashi Sugiyama for carrying out some of the experiments.

References

1) G. Kreysa, S. Pionteck, and E. Heitz, *J. Appl. Electrochem.*, **5**, 305 (1975).
2) G. Kreysa, *Electrochim. Acta*, **25**, 813 (1980).
3) S. Morooka and Y. Kato, *Kagaku Kohgaku*, **44**, 611 (1980).
4) Z. Ogumi, *Kagaku*, **34**, 316 (1978).
5) A. Tasaka, A. Itani, M. Koyama, and Y. Ohnishi, *Denki Kagaku*, **49**, 623 (1981).
6) M. Fleischmann, J. W. Oldfield, and D. F. Porter, *J. Electroanal. Chem.*, **29**, 244 (1971).
7) B. J. Sabacky and J. W. Evans, *J. Electrochem. Soc.*, **126**, 1182 (1979).
8) F. Hine, "Denki Kagaku Hanno Sousa to Denkaiso Kohgaku," Kagakudojin, Kyoto (1979), p. 68.
9) A. T. S. Walker and A. A. Wragg, *Chemical Engineering Science*, **35**, 405 (1980).
10) J. V. Zee and J. Newman, *J. Electrochem. Soc.*, **124**, 707 (1977).